Journal of Global Change Data & Discovery. 2021, 5(1): 45-53
DOI:10.3974/geodp.2021.01.06
www.geodoi.ac.cn

Dataset of Terrestrial Water Storage and Its Response to ENSO in the Three Parallel Rivers Basin (2002–2016)

Zhu, Y.[1,2] Liu, S. Y.[1,2*] Yi, Y.[1,2] Xie, F. M.[1,2]

1. Institute of International Rivers and Eco-Security, Yunnan University, Kunming 650091, China;
2. Yunnan Key Laboratory of International Rivers and Transboundary Eco-security, Kunming 650091, China

Abstract: The Three Parallel Rivers Basin (TPRB) is characterized by rough terrain and variable climate. The significant water cycle heterogeneity in the TPRB can be captured by the change in terrestrial water storage (TWS). In this dataset, the boundary of the TPRB was extracted based on the SRTM (30 m), integrated with the GloRiC dataset, Google Earth images, and related research results. The TWS in the TPRB was retrieved using the GRACE RL06 GSM monthly gravity field model from 2002 to 2016, and the results were corrected using a double-scale factor. The relationship between ENSO and TWS was quantified by linear fitting. The dataset includes: (1) the boundary of the TPRB (.shp); (2) spatiotemporal variation data of TWS, including the retrieved water reserves and model results for comparison (.nc); and (3) response data of TWS to ENSO (.nc). The data in (2) and (3) are archived in fifteen layers and different dimensions (one, two, or three dimensions) in NetCDF with monthly data in 1°x 1° spatial resolution. The dataset is archived in two data files with data size of 1.69 MB.

Keywords: TPRB; TWS; ENSO; 2002–2016

Dataset Availability Statement:

The dataset supporting this paper was published and is accessible through the *Digital Journal of Global Change Data Repository* at: https://doi.org/10.3974/geodb.2020.08.12.V1.

1 Introduction

The Three Parallel Rivers Basin (TPRB) is located in the transitional area between the eastern Qinghai–Tibet Plateau and the Yunnan–Guizhou Plateau, with large topographic relief, a complex climate background, and significant heterogeneity in the water cycle. The TPRB, as an important World Natural Heritage site, has attracted much attention to its hydrological processes, climate change, and ecological protection. In the context of global warming, fre-

Received: 01-12-2020; **Accepted:** 21-01-2020; **Published:** 25-03-2021
Foundations: National Natural Science Foundation of China (41761144075); Chinese Academy of Sciences (2019QZKK0208); Yunnan University (YJRC3201702)
***Corresponding Author:** Liu, S. Y. AAT-4278-2020, Institute of International Rivers and Eco-Security, shiyin.liu@ynu.edu.cn
Data Citation: [1] Zhu, Y., Liu, S. Y., Yi, Y., *et al.* Dataset of terrestrial water storage and its response to ENSO in the Three Parallel Rivers Basin (2002–2016) [J]. *Journal of Global Change Data & Discovery*, 2021, 5(1): 45–53. https://doi.org/10.3974/geodp.2021.01.06.
[2] Zhu, Y., Liu, S. Y., Yi, Y., *et al.* Dataset of terrestrial water storage and its response to ENSO in the Three Parallel Rivers Basin [J/DB/OL]. *Digital Journal of Global Change Data Repository*, 2020. https://doi.org/10.3974/geodb.2020.08.12.V1.

quent natural disasters have posed serious threats to economic production, life, and tourism development in this region[1]. In recent years, the frequent natural disasters in this area have mainly been large-scale droughts and floods. Some studies have pointed out that anomalies in the terrestrial water cycle are the primary reason for the occurrence of droughts and floods[2–4]. Anomalous changes in terrestrial water storage (TWS) can be used to effectively identify and monitor drought and flood events, and to link climate change with these events. Therefore, a dataset of spatiotemporal variations in TWS in the TPRB has important practical significance for the assessment of regional drought and flood disasters and the clarification of regional water cycle characteristics.

TWS can be obtained by site monitoring and model simulation. The former is limited by terrain conditions and costs, and continuous monitoring results are difficult to obtain, while the latter depends on the verification of observations. In contrast, retrieving TWS from remote sensing data shows great application potential[5]. Many scholars have applied Gravity Recovery and Climate Experiment (GRACE) data to carry out numerous studies on topics including drought monitoring, groundwater inversion, water storage and discharge effects of large reservoirs, and contributions of ice/snow melting to sea level changes[6,7]. GRACE data has great potential for monitoring global water storage since its spatial resolution is continuously improved in the follow-up satellite plans such as GRACE-Fo (GRACE Follow On)[7].

Meteorological factors play an important role in the water cycle. They show that extreme climate events such as the El Nino–Southern Oscillation (ENSO) can influence precipitation and induce temperature anomalies by affecting the atmospheric circulation, and eventually lead to regional and even global water storage anomalies, resulting in extreme drought and flooding[8]. The interannual variations of TWS in most regions of the world have a strong correlation with ENSO[9], and this is especially so for the TWS anomalies in some regions fully dominated by ENSO[10]. Therefore, it is necessary to consider the impact of ENSO on TWS, especially in such special areas as the TPRB.

2 Metadata of the Dataset

The metadata of the Dataset of terrestrial water storage and its response to ENSO in the Three Parallel Rivers Basin[11] is summarized in Table 1.

3 Methods for Data Production Development

3.1 Watershed Boundary Data

The boundary of the basin was extracted from SRTM with a spatial resolution of 30 m based on the pysheds (http://mattbartos.com/pysheds/) and the Google Earth platform. The specific steps are as follows.

The pysheds[1] was used to conduct operations including filling, flow direction, and flow routing on SRTM data.

The preliminary boundary was extracted based on the results of step (1) and the outlet, which was determined by prior studies and the requirement to avoid the impact of reservoirs in the middle and lower reaches.

[1] pysheds. http://mattbartos.com/pysheds/.

Table 1 Metadata summary of the Dataset of terrestrial water storage and its response to ENSO in the Three Parallel Rivers Basin

Items	Description
Dataset full name	Dataset of terrestrial water storage and its response to ENSO in the Three Parallel Rivers Basin
Dataset short name	TWS_ENSO_TPRB
Authors	Zhu Y. ABD-2058-2020, Institute of International Rivers and Eco-Security, Yunnan University, yuzhu@mail.ynu.edu.cn Liu S. Y. AAT-4278-2020, Institute of International Rivers and Eco-Security, shi-yin.liu@ynu.edu.cn Yi Y. ABD-3176-2020, Institute of International Rivers and Eco-Security, yin-gyi@mail.ynu.edu.cn Xie F. M. ABD-3175-2020, Institute of International Rivers and Eco-Security, xfm@mail.ynu.edu.cn
Geographical region	27°N–36°N, 90°E–101°E Year Aug. 2002–Sep. 2016
Time resolution	1 month Spatial resolution 1°
Data format	.shp, .nc Data size 1.69 MB
Data files	(1) boundary of the TPRB (TPRB.shp) (2) TWS and its associated data (TPRB_TWS_ENSO_2002-2016.nc)
Foundations	National Natural Science Foundation of China (41761144075); Chinese Academy of Sciences (2019QZKK0208); Yunnan University (YJRC3201702)
Computing environment	Python 3.7
Data publisher	Global Change Research Data Publishing & Repository, http://www.geodoi.ac.cn
Address	No. 11A, Datun Road, Chaoyang District, Beijing 100101, China
Data sharing policy	***Data*** from the Global Change Research Data Publishing & Repository includes metadata, datasets (in the *Digital Journal of Global Change Data Repository*), and publications (in the *Journal of Global Change Data & Discovery*). ***Data*** sharing policy includes: (1) ***Data*** are openly available and can be free downloaded via the Internet; (2) End users are encouraged to use ***Data*** subject to citation; (3) Users, who are by definition also value-added service providers, are welcome to redistribute ***Data*** subject to written permission from the GCdataPR Editorial Office and the issuance of a ***Data*** redistribution license; and (4) If ***Data*** are used to compile new datasets, the 'ten percent principal' should be followed such that ***Data*** records utilized should not surpass 10% of the new dataset contents, while sources should be clearly noted in suitable places in the new dataset[12]
Communication and searchable system	DOI, DCI, CSCD, WDS/ISC, GEOSS, China GEOSS, Crossref

Obvious inconsistencies between the initial boundary and the boundary found by GloRiC[13][2] were marked. The boundaries in the water outlet area, the glacier/snow-covered area, the deep ridge and valley area, and especially the marked area in (3) were checked and modified under the condition of a viewing altitude of 1–2 km on the Google Earth platform to obtain a final accurate boundary of the TPRB.

3.2 Inversion of TWS

The GRACE LEVEL-2 (RL06) GSM[3] monthly gravity field model from August 2012 to August 2016, released by the Center for Space Research, University of Texas at Austin (UTCSR), was employed in this study. The procedures for deriving TWS from GRACE are shown as follows.

(1) Data preprocessing

It is necessary to filter the GRACE solutions to reduce the introduction of errors in original data. The errors that must be processed mainly include the C20 of GRACE, the north–south strips, and the errors in the high-order spherical harmonic coefficient. Generally, the GRACE C20 data were replaced by SLR C20 data, which include more seasonal characteristics, and the other two errors were primarily removed by filtering[14]. The specific pro-

[2] WWF. HydroSHEDS database. https://www.hydrosheds.org/page/development.
[3] CSR GRACE/GRACE-FO RL06 Mascon Solutions (version 02). http://www2.csr.utexas.edu/grace/RL06_mascons.html.

cessing flow is shown in Figure 1.

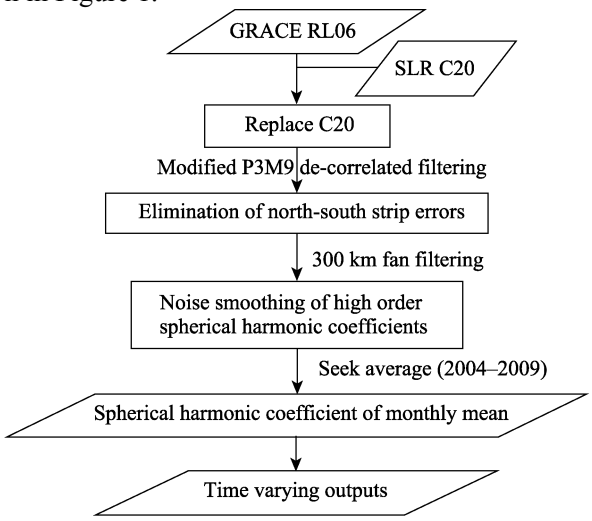

Figure 1 Flow chart of data preprocessing

(2) Conversion of gravity signal

Generally, the change in TWS is expressed by Equivalent Water Thickness (EWT). The change in TWS will cause a change in the spherical gravity field[15]. Based on this theory, the gravity signal of a certain point (θ, λ) in the earth can be converted into the change signal of TWS (Δh) through Equation (1)[16]:

$$\Delta h(\theta,\lambda)=\frac{R\rho_e}{3\rho_w}\sum_{n=0}^{N}\frac{2n+1}{1+k_n}W_n\sum_{m=0}^{n}W_m(\Delta C_{nm}\cos m\lambda+\Delta S_{nm}\sin m\lambda)\bar{P}_{nm}(\cos\theta) \quad (1)$$

where R represents the mean radius of the earth; (θ,λ) refer to the geocentric latitude and longitude of the calculation points, respectively; ρ_e is the average density of the earth; ρ_w is the average density of water; k_n denotes the loading Love numbers; both ΔC_{nm} and ΔS_{nm} are normalized spherical harmonic coefficients; $\bar{P}_{nm}(\cos\theta)$ indicates the normalized m order n multiplied by the Legendre function; and N is the order of the spherical harmonic coefficients. Studies have identified significant errors in the higher-order terms. As a result, the higher-order terms usually must be truncated (generally, N=60)[17–19]. Both W_n and W_m are Gaussian filtering smoothing functions. When $r_{1/2}$ represents the filter radius, the Gaussian kernel function W is calculated using Equation (2).

$$W_0=\frac{1}{2\pi},W_1=\frac{1}{2\pi}\left(\frac{1+e^{-2\alpha}}{1-e^{-2\alpha}}-\frac{1}{\alpha}\right),\ldots,W_{n+1}=-\frac{2n+1}{\alpha}W_n+W_{n-1}\ \ (n>2) \quad (2)$$

(3) Recovery of the attenuated signal amplitude

Although preprocessing can effectively reduce the errors in the original data, it inevitably leads to the attenuation of the gravity signal amplitude. In data production, the double-scale factor method was used to recover the amplitude signal (see reference [5] for the specific content). The processing steps were as follows:

a) The spherical harmonic expansion of the GLDAS TWS was calculated (the expansion order is the same as for GRACE, and is here the 60th order).

b) The same postprocessing procedures used for GRACE data were conducted on the spherical harmonic coefficient of the GLDAS TWS.

c) The normalized spherical harmonic coefficients before and after preprocessing were used to calculate the corresponding EWT PP_T and AP_T in the study area, respectively.

d) The trend items (PP_{T1} and AP_{T1}) and the seasonal items (PP_{T2} and AP_{T2}) were acquired by using STL[20–22] to decompose the PP_T and AP_T .

e) The regional scale factors (S_1 and S_2) were calculated according to the principle of minimizing the sum of squares of residual errors for the time series (including the trend term and seasonal term) before and after processing, that is, $\sum(PP_{Ti} - S_i \cdot AP_{Ti})^2$ $(i = 1, 2)$ is the minimum.

f) Two scale factors were used to recover the seasonal term and trend term, respectively, and finally, we obtained the recovered TWS via the inverse calculation of STL.

3.3 Quantification of the Relationship Between TWS and ENSO

A linear fitting method was used to quantify the response mechanism of TWS to ENSO[23–24]. First, STL decomposition was used to obtain the effective signal of TWS change ($TWSC_{residuals}$); then, Equation (3) was used to fit the relationship between the effective signal and ENSO, and the fitting coefficients (a, b, and c) were calculated. Finally, the amplitude (AMP) and phase lag (Phase) were calculated by Equation (4). The $imag(Hilbert(MEI))$ term gives the imaginary part of the ENSO index MEI by the Hilbert transform.

$$TWSC_{residuals} = a + b \times \mathrm{MEI} + c \times imag(Hilbert(MEI)) \tag{3}$$

$$\begin{cases} AMP = sqrt(b^2 + c^2) \\ Phase = tan^{-1}\left(\dfrac{c}{b}\right) \end{cases} \tag{4}$$

4 Data Results and Validation

4.1 Components of the Dataset

The content of the dataset is consisted of three parts, including: (1) the boundary of TPRB (.shp); (2) spatiotemporal variation data of TWS, including the retrieved water reserves and model results for comparison (.nc); (3) response data of TWS to ENSO (.nc). The data in (2) and (3) are archived in fifteen layers and different dimensions (one, two or three dimension) in NetCDF with monthly data in 1°×1° spatial resolution. The detailed description of the dataset is shown in Table 2.

4.2 Data Analysis

Figures 2 (a) and 2 (b) show the spatial variations of TWS. There is a significant spatial heterogeneity that exhibits a downward trend in the southwest and an upward trend in the northwest. The most obvious decline took place in the Nujiang River Basin. The TWS in the headwater area of the TPRB increased. From 2002 to 2016, the TWS in the TPRB showed an obvious downward trend with clear characteristics of seasonal variation (Figure 2(c)). From the fluctuation of residuals in TWS, anomalous signals are evident in the springs of 2003 and 2004 and the winters of 2006 and 2015, which indicate that drought (flood) disasters occurred in these periods. Figure 3 shows the effect of ENSO on regional water storage. In general, the impact intensity of ENSO on regional TWSC is 0.95 mm per month, and the response time lag of TWS to ENSO is 2.72 months. A comparison of Figure 2(a) and Figure 3 shows that the loss of water reserves is more serious in the regions with large ENSO impacts on TWS, especially in the Nujiang River Basin.

Table 2 Descriptions of the dataset files

Data name	Data properties					Data size
	Variable	Time range	Frequency	Resolution	Descriptions	
TPRB.shp	–	–	–	–	The boundary extracted from SRTM and corrected in the Google Earth platform	1.49 MB
TPRB_TWS_ENSO_2002-2016.nc*	EWT	Aug.1, 2002–Sep.1, 2002	monthly	1°	Gridded equivalent water thickness derived from GRACE	208.0 KB
	TWS_grace_t TWS_noah_t TWS_cpc_t	Aug.1, 2002–Sep.1, 2002	monthly	–	The temporal TWS derived from GRACE, GLDAS-NOAH, and CPC, respectively, which are used for analysis and calculation of the double-scale factor	
	TWS_gra_trend TWS_gra_season TWS_gra_residual	Aug.1, 2002–Sep.1, 2002	monthly	–	The trend, seasonality, and residuals of TWS derived from GRACE	
	TWS_rate_spa	–	–	1°	The change rate of TWS in the TPRB	
	SM GW SW CW SR	Aug.1, 2002–Sep.1, 2002	monthly	–	The components in TWS. Soil moisture (SM), canopy water (CW), and snow water (SW) were derived from GLDAS-NOAH[25]; groundwater (GW) was derived from WGHM[26]; Surface runoff (SR) was derived from GRUN[27]	
	enso_amp	–	–	1°	Influence magnitude of ENSO on TWS	
	enso_phase	–	–	1°	The time-lag of influence between ENSO and TWS	

* The dataset is stored in netCDF format with multiple layers and different dimensions. The attributes in each layer include unit, description, reference, etc. The attributes of the dataset include coordinate system, projection, resolution, processing program, and other related information.

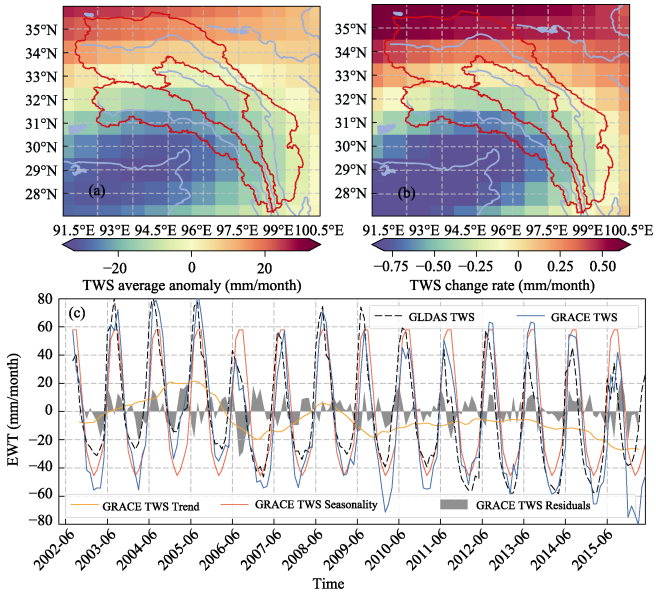

Figure 2 Map of TWS derived from GRACE. (a) Spatial characteristics of the TWS anomaly; (b) change rate of TWS; (c) temporal changes in TWS and its components

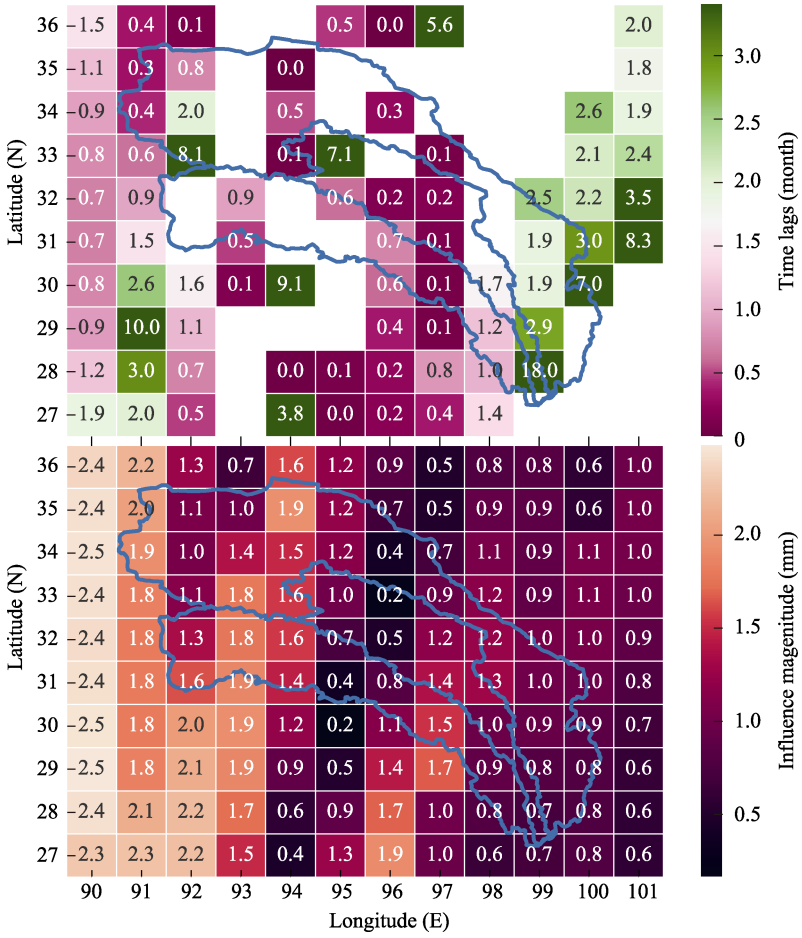

Figure 3 Influence magnitude of ENSO on TWS and time-lag of the responses

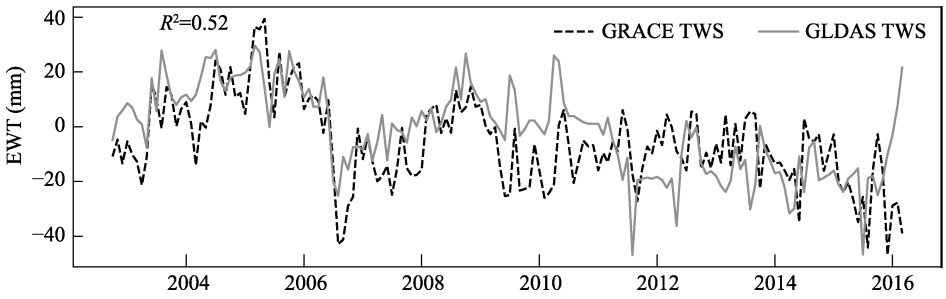

Figure 4 Time variations of non-seasonal TWS derived from GRACE and GLDAS

4.3 Data Validation

Generally, the main component of regional water storage is soil moisture. GLDAS presents a good simulation reflecting soil moisture. We therefore used TWS derived from GLDAS to validate the TWS derived from GRACE. It can be seen in Figure 4 that the two time series show good consistency for temporal changes (R^2 is 0.86 ($P< 0.0001$); R^2 between time series with seasonal changes removed is 0.52 ($P< 0.0001$)). In addition, the station-based TWS

calculated from the perspective of water balance was also used to validate the GRACE TWS. The results showed that the magnitude and variation trend of the inversion results were consistent with the measured TWS (see chapter 4.1 in reference [5]), although it is difficult to capture the small time-varying characteristics in the GRACE TWS.

5 Discussion and Summary

In this paper, the TWS in the TPRB was derived from GRACE RL06 time-varying gravity field data. The spatiotemporal characteristics of TWS were decomposed and analyzed by statistical methods, and the impact of ENSO on the changes of TWS was quantified. Our research dataset is helpful for the monitoring and research of the water cycle in this region.

The spatial resolution of the TWS derived from GRACE is relatively coarse (1 ° × 1 °), which is mainly determined by the characteristics of the gravity satellite. Therefore, although the results in this dataset can better reflect the variations of TWS, the uncertainty of the results will increase significantly when analyzing the TWS in a small area. For this situation, our results need to be evaluated using station observations or meteorological data from high-resolution satellite observations.

This dataset can simply reveal water cycle processes in the TPRB and can be used to analyze the causes of water storage changes in the context of extreme climate events. However, in high-altitude areas (mainly source areas), due to the uncertainty of the glacier and snow meltwater, the contribution of each component to the TWS will be affected. Therefore, the seasonal variations of glacier melt and snowmelt and the water level change of lakes should be considered when analyzing the TWS changes over these areas.

This dataset includes not only the data related to water storage but also the basin boundary of the TPRB, which could be useful in future studies of this region.

Author Contributions

Liu, S. Y. and Zhu, Y. designed the algorithms and research framework of the dataset. Yi, Y. contributed to collecting and processing the GRACE solutions. Xie, F. M. evaluated the data. Zhu, Y. wrote the data paper and Liu, S. Y. reviewed the paper. The authors declare no conflicts of interest.

Conflicts of Interest

The authors declare no conflicts of interest.

References

[1] Luo, Y. H., Zhou, D. Y., Zhu, R. H., *et al*. Primary study on environment of geology and bionomics in the area of world natural inheritance-the three rivers juxtaposition [J]. *Journal of Geological Hazards and Environment Preservation*, 2008, 19(2): 94–97.

[2] Chen, X., Jiang, J., Li, H. Drought and flood monitoring of the liao river basin in northeast China using extended GRACE data [J]. *Remote Sensing*, 2018, 10(8): 1168.

[3] Schumacher, M., Forootan, E., Van, D. A. I. J. M., *et al*. Improving drought simulations within the Murray-Darling Basin by combined calibration/assimilation of GRACE data into the WaterGAP Global Hydrology Model [J]. *Remote Sensing of Environment*, 2018, 204(1): 212–228.

[4] Chen, J. L., Wilson, C. R., Tapley, B. D., *et al*. 2005 drought event in the Amazon River basin as measured by GRACE and estimated by climate models [J]. *Journal of Geophysical Research*, 2009, 114(B5): B05404.

[5] Zhu Y., Liu S. Y., Yi, Y., *et al*. Spatiotemporal changes of terrestrial water storage in three parallel river basins and its response to ENSO [J]. *Mountain Research*, 2020, (2): 165–179.

[6] Feng, W., Wang, C. Q., Mu, D. P., *et al*. Groundwater storage variations in the North China Plain from GRACE with spatial constrains [J]. *Chinese Journal of Geophysics*, 2017, 60(5): 1630–1642.
[7] Tapley, B. D., Watkins, M. M., Flechtner, F., *et al*. Contributions of GRACE to understanding climate change [J]. *Nature Climate Change*, 2019, 9: 358–369.
[8] Zhang, Z., Chao, B. F., Chen, J., *et al*. Terrestrial water storage anomalies of Yangtze River Basin droughts observed by GRACE and connections with ENSO [J]. *Global and Planetary Change*, 2015, 126(1): 35–45.
[9] Ni, S., Chen, J., Wilson, C. R., *et al*. Global Terrestrial Water Storage Changes and Connections to ENSO Events [J]. *Surveys in Geophysics*, 2018, 39(1): 1–22.
[10] Jin, Z. W., Jin, T. Y. Correlation between ENSO and Total water storage change anomaly with extreme weather events over Amazon basin from 2010 to 2016 estimated from GRACE and hydroclimatic data [J]. *Journal of Geodesy and Geodynamics*, 2019, 39(2): 93–97.
[11] Zhu, Y., Liu, S. Y., Yi, Y., *et al*. Dataset of terrestrial water storage and its response to ENSO in the Three Parallel Rivers Basin [J/DB/OL]. *Digital Journal of Global Change Data Repository*, 2020. https://doi.org/10.3974/geodb.2020.08.12.V1.
[12] GCdataPR Editorial Office. GCdataPR data sharing policy [OL]. https://doi.org/10.3974/dp.policy.2014.05 (Updated 2017).
[13] Dallaire, C. O., Lehner, B., Sayre, R., *et al*. A multidisciplinary framework to derive global river reach classifications at high spatial resolution [J]. *Environmental Research Letters*, 2018, 14(2): 024003.
[14] Han, S. C., Shum, C. K., Jekeli, C., *et al*. Non-isotropic filtering of GRACE temporal gravity for geophysical signal enhancement [J]. *Geophysical Journal International*, 2005, 163(1): 18–25.
[15] Tapley, B. D., Bettadpur, S., Watkins, M., *et al*. The gravity recovery and climate experiment: Mission overview and early results [J]. *Geophysical Research Letters*, 2004, 31(9): L09607.
[16] Wahr, J., Molenaar, M., Bryan, F. Time variability of the Earth's gravity field: Hydrological and oceanic effects and their possible detection using GRACE [J]. *Journal of Geophysical Research*: *Solid Earth*, 1998, 103(B12): 30205–30229.
[17] Longuevergne, L., Scanlon, B. R., Wilson, C. R. GRACE Hydrological estimates for small basins: Evaluating processing approaches on the High Plains Aquifer, USA [J]. *Water Resources Research*, 2010, 46(11): 6291–6297.
[18] Feng, W., Zhong, M., Lemoine, J. M., *et al*. Evaluation of groundwater depletion in North China using the Gravity Recovery and Climate Experiment (GRACE) data and ground-based measurements [J]. *Water Resources Research*, 2013, 49(4): 2110–2118.
[19] Swenson, S., Wahr, J. Post-processing removal of correlated errors in GRACE data [J]. *Geophysical Research Letters*, 2006, 33(8): L08402.
[20] Rojo, J., Rivero, R., Romero-morte, J., *et al*. Modeling pollen time series using seasonal-trend decomposition procedure based on LOESS smoothing [J]. *International Journal of Biometeorology*, 2017, 61(2): 335–348.
[21] Sanchez-vazquez, M. J., Nielen, M., Gunn, G. J., *et al*. Using seasonal-trend decomposition based on loess (STL) to explore temporal patterns of pneumonic lesions in finishing pigs slaughtered in England, 2005–2011 [J]. *Preventive Veterinary Medicine*, 2012, 104(1/2): 65–73.
[22] Cleveland, R. B., Cleveland, W. S. STL: a seasonal-trend decomposition procedure based on loess [J]. *Journal of Official Statistics*, 1990, 6(1): 3–33.
[23] Phillips, T., Nerem, R. S., Fox-kemper, B., *et al*. The influence of ENSO on global terrestrial water storage using GRACE [J]. *Geophysical Research Letters*, 2012, 39(16): L16705.
[24] Salisbury, J. I., Wimbush, M. Using modern time series analysis techniques to predict ENSO events from the SOI time series [J]. *Nonlinear Processes in Geophysics*, 2002, 9(4): 341–345.
[25] Rodell, M., Houser, P. R., Jambor, U., *et al*. The global land data assimilation system [J]. *Bulletin of the American Meteorological Society*, 2004, 85(3): 381–394.
[26] Döll, P., Schmied, H. M., Schuh, C., *et al*. Global-scale assessment of groundwater depletion and related groundwater abstractions: combining hydrological modeling with information from well observations and GRACE satellites [J]. *Water Resources Research*, 2015, 50(7): 5698–5720.
[27] Ghiggi, G., Humphrey, V., Seneviratne, S. I., *et al*. GRUN: an observations-based global gridded runoff dataset from 1902 to 2014 [J]. *Earth System Science Data*, 2019, 11(4): 1655–1674.